THE ANATOLIAN JOURNAL OF CARDIOLOGY

Official journal of the TURKISH SOCIETY OF CARDIOLOGY

T1 Mapping in Differentiating Healthy and Pathological Myocardium

ORIGINAL INVESTIGATION

ABSTRACT

Background: This study aimed to identify the optimal measurement location and technique for native T1 mapping to establish a standardized approach. The diagnostic performance of various T1 mapping measurement approaches was evaluated by comparing nonischemic dilated cardiomyopathy (NIDCM) and hypertrophic cardiomyopathy (HCM) cohorts with a control group.

Methods: Patients who underwent 1.5 T cardiac magnetic resonance (CMR) were retrospectively reviewed with standardized protocol [functional sequences, T1 mapping, and late gadolinium enhancement] between November 2016 and January 2023. A total of 143 subjects (61 NIDCM, 60 HCM, and 22 controls) were grouped based on CMR findings. Native T1 mapping images were acquired in basal, midventricular, and apical short-axis (SAX) slices. Regions of interest were drawn in both the whole left ventricular (LV) myocardium SAX and the interventricular septum. Diagnostic yield and optimal cut-off values for native T1 were investigated.

Results: Native T1 values were significantly higher than the control group for 6 different measurement approaches ($P < .05$). Basal SAX and basal septal measurements provided the highest diagnostic accuracy values for both groups. Statistical analysis revealed that T1 values could differentiate between healthy and diseased myocardium, with a diagnostic accuracy of 86% for NIDCM and 73.4% for HCM. Furthermore, T1 values correlated with measures of global systolic function and LV remodeling.

Conclusions: The study shows that native T1 mapping using a streamlined single-slice acquisition with a septal measurement technique achieves diagnostic performance comparable to multi-slice protocols while reducing measurement heterogeneity. This optimization facilitates a time-efficient workflow and improves patient comfort without compromising diagnostic accuracy.

Keywords Cardiac diseases, cardiomyopathies, fibrosis, magnetic resonance imaging, T1 mapping

INTRODUCTION

Cardiac magnetic resonance (CMR) T1 mapping is a technique for quantitative assessment of tissue characteristics in cardiac disease and provides a unique assessment of diffuse fibrosis in various cardiomyopathies. In recent years, it has been recognized that the myocardial interstitium has an important role in the pathogenesis of long-term cardiovascular complications, mainly heart failure.[1-6] The accumulation of fibrillar collagen in the highly organized architecture of the myocardial interstitial space, known as myocardial fibrosis, has been identified as a major cause of myocardial dysfunction. From a histopathological point of view, myocardial fibrosis can be classified as "focal" confined to a definable area, and "diffuse," which is more uniform, with a global distribution.[2-6] Diffuse myocardial fibrosis, which leads to myocardial remodeling, is the fundamental process in the development of myocardial dysfunction in several cardiomyopathies.[1-2,7] Recent clinical studies have also shown that fibrosis is an important independent predictor of adverse cardiac outcomes.[3]

Cardiac magnetic resonance is a non-invasive imaging modality that provides a comprehensive assessment of myocardial anatomy and function with high accuracy and reproducibility. Late gadolinium enhancement (LGE) imaging and

Sena Bozer Uludağ
Sena Ünal
Elif Peker
Çağlar Uzun

Department of Radiology, School of Medicine, Ankara University, Ankara, Türkiye

Corresponding author:
Çağlar Uzun
✉ cuzun77@yahoo.com

Received: January 5, 2026
Accepted: March 24, 2026
Available Online Date: May 22, 2026

Cite this article as: Uludağ SB, Ünal S, Peker E, Uzun Ç. T1 mapping in differentiating healthy and pathological myocardium. *Anatol J Cardiol.* 2026;30(6):386-400.

DOI: 10.14744/AnatolJCardiol.2026.6183

T1 mapping are the 2 main CMR techniques used for myocardial fibrosis assessment. The visualization of fibrosis by CMR is based on the expansion of the extracellular space due to fibrosis, resulting in an increased volume of gadolinium distribution and delayed washout within the tissue.[6-8] Visualization of cardiac pathology with LGE relies on differential spatial accumulation of gadolinium to provide black-and-white image contrast. Therefore, focal fibrosis is easily distinguished by well-demarcated areas, whereas diffuse fibrotic processes cannot be sufficiently visualized as abnormal patterns, because there is no apparent contrast between 1 region and another.[6-7,9] T1 mapping is a technique that enables the diagnosis of these diffuse conditions by measuring T1 values that directly correspond to the variation in intrinsic tissue properties involving the entire myocardium. Several studies have proposed that native T1 values are potentially valuable for the quantitative assessment of myocardial fibrosis, which can be used for the assessment of disease activity, the follow-up of disease progression, and guiding treatment.[1,3,7,10-12] Native T1 mapping also has additional benefits in patients who cannot tolerate a prolonged CMR scan or who have contraindications to the use of contrast media, mainly renal impairment and a history of allergic or anaphylactic reaction, which prohibit obtaining LGE sequences.[6,13]

Current literature describes different approaches to myocardial T1 measurements ranging from segmental models to the entire myocardium within the short axis (SAX) plane. The Society for Cardiovascular Magnetic Resonance (SCMR) and the European Association of Cardiovascular Imaging (EACVI) consensus statement recommends drawing a single region of interest (ROI) in the mid-cavity septum for assessing diffuse disease to minimize susceptibility artifacts and partial volume effects.[10] However, there is still limited comparative data on whether other anatomical levels might offer superior diagnostic accuracy or better reproducibility in different cardiomyopathy phenotypes. Further comparative data are needed to establish a robust, standardized, and time-efficient measurement approach for routine clinical practice.

The present study aimed to evaluate the performance of native T1 mapping with modified Look-Locker inversion recovery (MOLLI) 5(3)3, between healthy and diffusely diseased myocardium in 2 different subgroups including nonischemic dilated cardiomyopathy (NIDCM) and hypertrophic cardiomyopathy (HCM). The primary objective was to identify the optimal anatomical level and measurement technique that provides the highest diagnostic accuracy. By comparing different approaches, the study aimed to demonstrate the most practical measurement method for routine clinical practice.

HIGHLIGHTS

- Native T1 mapping effectively distinguishes healthy myocardium from diffuse disease and enables early detection of disease in nonischemic dilated cardiomyopathy and hypertrophic cardiomyopathy patients without the need for contrast agents.
- Although basal levels provided the numerically highest area under the curve values, no statistically significant difference was observed between ventricular levels, supporting that a single-slice acquisition alone provides diagnostic performance comparable to multi-slice protocols.
- The septal measurement technique offers significantly lower measurement heterogeneity than whole-slice short axis approaches.
- A streamlined single-slice protocol offers a feasible approach to improving clinical workflow by reducing scan time and enhancing patient comfort by minimizing breath-holding burden.
- Increased native T1 values correlate significantly with impaired global systolic function and left ventricular remodeling.

METHODS

Ethics and Study Population

This retrospective case-control study protocol was approved by the approved by the Institutional Human Research Ethics Committee of Ankara University (Approval No: I01-65-24, dated February 6, 2024), and written informed consent was obtained from all participants.

Between November 2016 and January 2023, patients who underwent 1.5 T CMR with standardized protocol for any clinical prediagnosis were retrospectively reviewed. Prior to enrollment, subjects were grouped based on CMR findings. Nonischemic dilated cardiomyopathy is defined as the presence of left ventricular (LV) dilation and systolic dysfunction, which can be measured as increased LV end-diastolic volume (EDV) and LV end-systolic volume (ESV) indexed to body surface area (BSA) (EDVi >100, ESVi > 37) and decreased LV ejection fraction (EF) (EF < 56%) that cannot be explained by coronary artery disease or abnormal stress in the absence of ischemic-like LGE.[14-18] Hypertrophic cardiomyopathy is defined as the presence of a maximal end-diastolic wall thickness (LVWTmax) of ≥15 mm in the absence of LV dilatation that cannot be explained by abnormal loading conditions.[15,16,19] In the presence of family members of a patient with HCM or association with a positive genetic test, more limited hypertrophy (13 mm) was considered diagnostic.[19,20] The control group consisted of normotensive subjects who had undergone unenhanced CMR throughout the study period, with normal CMR findings. Selecting these individuals from the same clinical workflow and timeframe as the patient groups enabled the creation of a longitudinally matched internal reference. This approach aimed to reduce potential fluctuations in T1 measurements, thereby ensuring comparability across the 7-year study period. The patient enrollment is shown in Figure 1. Patients were excluded if they had evidence of 1) ischemic type LGE; 2) myocardial infiltration due to amyloidosis, iron accumulation, lipid-storage disease, arrhythmogenic right ventricular cardiomyopathy; or 3) significant primary valvular heart disease, based on CMR findings. Also, patients with incomplete CMR sequences or artifacts that cause contaminated nondiagnostic images

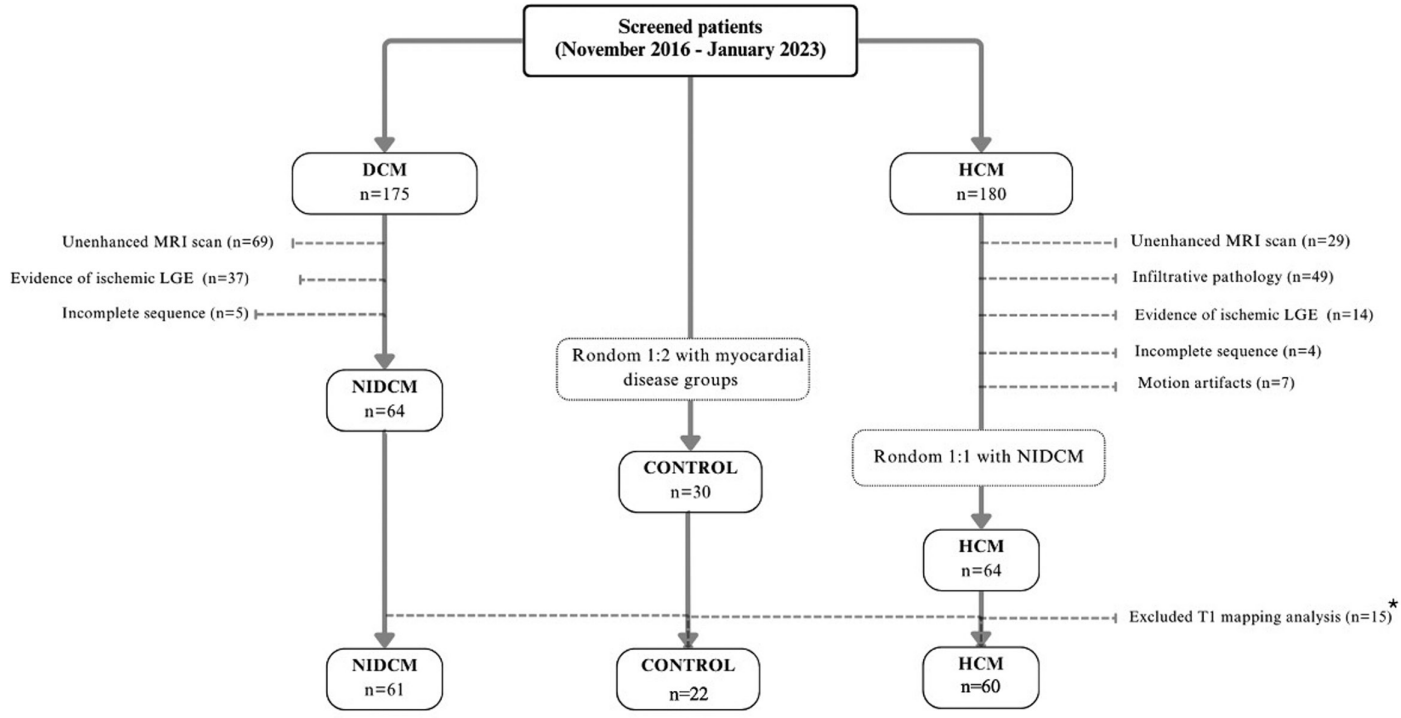

Figure 1. The patient enrollment and group assignment protocol. *Three patients with only basal T1 mapping slices, 9 patients with severe uncorrectable respiratory and motion artifacts, and 3 patients with LVOT on basal section images, a total of 15 patients were excluded. DCM, dilated cardiomyopathy; HCM, hypertrophic cardiomyopathy; LGE, late gadolinium enhancement; LVOT, left ventricle outflow tract; MRI, magnetic resonance imaging; NIDCM, nonischemic dilated cardiomyopathy.

served as exclusion criteria. Furthermore, patients with T1 mapping images showing the LV outflow tract (LVOT) at the basal level were excluded to avoid partial volume effects and measurement contamination in the septum (Figure 2). Patients in the HCM group were randomly selected to match the number of patients in the NIDCM group. Patients in the control group were also randomly selected to have half of the sample size of the cardiomyopathy groups.

Cardiac Magnetic Resonance Protocol and Image Analysis

The CMR examinations were performed using a 1.5 T magnetic resonance imaging (MRI) scanner (Aera, Siemens Healthcare), and 18-channel cardiac coil with standardized protocol and post-processing procedures.

Cine short axis and long axis images were acquired by retrospective gating and breath holding in expiration, with parallel imaging performed using a balanced steady-state free precession technique (repetition time/time to echo (TR/TE), 42.98/1.33; flip angle, 80°).

T1 mapping images were obtained using MOLLI 5(3)3 heart rate–corrected sequence, in the SAX, through the basal, mid-ventricular, and apical slices obtained in the mid-diastole, as previously described.[21,22] To obtain the same slice position at the basal section for each patient, the basal slice was standardized using the 5′ in 3′ method as previously described.[23] Magnetic resonance imaging parameters for T1 mapping were TR: 272 ms, TE: 1.12 ms, field of view (FOV) 360 × 360 mm, inversion time (TI) 180 ms, slice thickness 8 mm, number of slices: 3. All mapping parameters remained unchanged throughout the 7-year study period to ensure longitudinal stability.

Late gadolinium enhancement images were obtained approximately 9-10 minutes after an intravenous injection of 0.1 mmol/kg of gadobutrol with TI selected according to the nulling time detected at Look-Locker images. Magnetic resonance imaging parameters for LGE were TR: 702 ms, TE: 1.09 ms, FOV: 340x340 mm, slice thickness: 8 mm, and number of slices: 3.

An imaging software workstation (syngo.via, Siemens Healthineers) was used to perform cardiac volume measurements. Simpson's rule was used to determine the global function of the left ventricle.[24] All volumes were normalized to BSA. Measurement of end-diastolic LV myocardial thickness on SAX images and LVWTmax was noted for all subjects.

T1 mapping measurements were performed on inline motion-corrected maps, using an imaging software workstation (syngo.via, Siemens Healthineers). To determine the optimal diagnostic approach, 6 distinct measurement datasets per patient were generated by drawing ROIs that cover the whole LV myocardium and the interventricular septum in the basal, mid-ventricular, and apical slices (Figure 3). These ROI placements were performed with high precision to exclude the blood pool and papillary muscles, thereby minimizing potential partial volume effects at the endocardial and epicardial borders. Reported T1 values were derived without looking at the corresponding LGE images. Mean and standard deviation (SD) values were noted. Coefficient

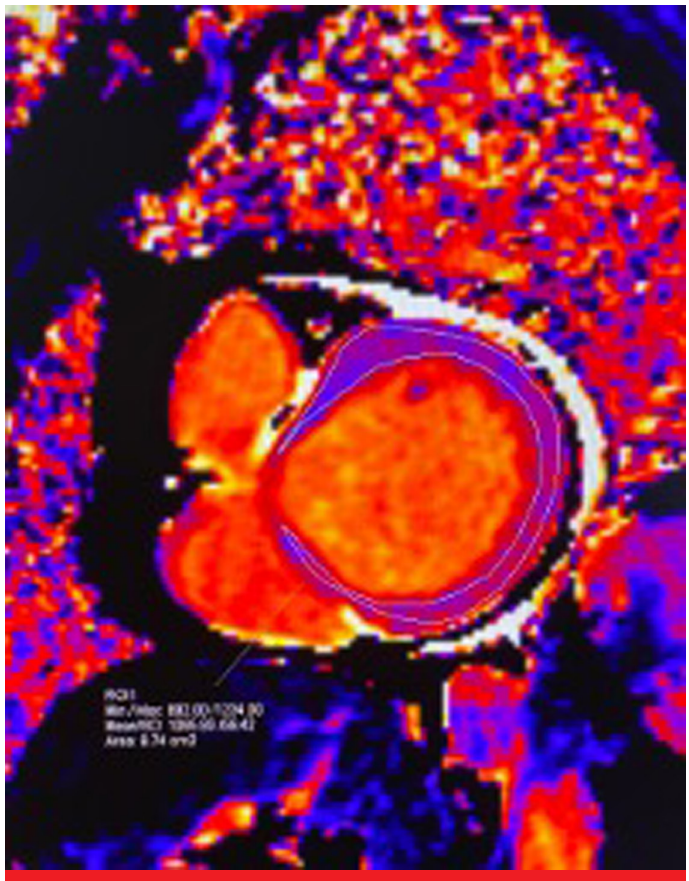

Figure 2. Basal section of the native T1 mapping. Septum was not included in the SAX measurement due to contamination and partial volume effects caused by the LVOT. In conclusion, patients with LVOT at the basal level were excluded from the study. LVOT, left ventricular outflow tract; SAX, short-axis.

of variation (CoV) reflecting the heterogeneity of T1 values was assessed by the formula: mean/SD.[25,26] T1 measurements were performed by a single observer (S.B.U., 3 years of experience in CMR) and randomly selected subjects were re-measured by the first observer to analyze intra-observer agreement and a second observer (E.P., 12 years of experience in CMR) to analyze inter-observer agreement.

Statistical Analysis

Statistical analyses were performed using SPSS software version 13.0 (IBM Corp., Armonk, NY, USA). The normality of continuous variables was assessed for each study group separately using the Shapiro–Wilk test. Descriptive statistics are presented as mean ± SD for continuous variables and as frequencies with percentages (%) for nominal data. Categorical data were compared using the Chi-square test or Fisher's exact test, as appropriate. For comparisons between 2 independent subgroups, the Student's *t*-test or Mann–Whitney *U*-test was employed. The paired *t*-test and Wilcoxon signed-rank test were utilized for paired comparisons of different measurement locations within each of the 3 study groups. For inter-group comparisons of continuous variables across the 3 study groups (control, NIDCM, and HCM), a one-way analysis of variance (ANOVA) with Tukey's Honestly Significant Difference post-hoc test was used for parametric data, while the Kruskal–Wallis test followed by Bonferroni-adjusted Dunn's test was used for non-parametric variables. Intra- and inter-observer agreements were evaluated using the intraclass correlation coefficient (ICC). The diagnostic performance of each measurement approach was determined through receiver operating characteristic (ROC) curve analysis. Comparison of the area under the curve (AUC) values was conducted using DeLong's test. The relationships between native T1 relaxation times and morphological or functional parameters were evaluated using Spearman's rank correlation analysis. Statistical significance was accepted for $P < .05$.

RESULTS

Study Population

A total of 143 subjects with NIDCM (n = 61), HCM (n = 60), and control group (n = 22) were enrolled in the study. Patients' demographic characteristics are shown in Table 1. There was no significant difference in age between NIDCM and HCM ($P = .159$). All groups had similar sex representations ($P = .658$), as well as body mass index (BMI) ($P = .095$) and BSA ($P = .292$).

Global Morphological and Functional Parameters

In comparison with the control group; patients with HCM had significantly higher LV-mass indices ($X^2(2) = 33.46$, $P < .001$) and increased LVWT ($X^2(2) = 105.71$, $P < .001$), and patients with NIDCM had enlarged cavity volumes (LV-ESVi: $X^2(2) = 102.78$, $P < .001$; LV-EDVi: $X^2(2) = 98.18$, $P < .001$) and lower EF ($X^2(2) = 95.26$, $P < .001$). Global morphological and functional measures for all patients are presented in Table 2.

Native T1 Values Across Different Measurement Approaches in Nonischemic Dilated Cardiomyopathy, Hypertrophic Cardiomyopathy, and Control Groups

The mean native myocardial T1 value in the control group was 997.67 ± 23.88 ms; in NIDCM group was 1053.52 ± 58.60 ms; in HCM group was 1029.97 ± 46.36 ms. The native T1 values of cardiomyopathies and controls are shown in Table 3. T1 values were significantly higher in 2 different cardiomyopathy groups than the control group for all measurement approaches ($P < .05$). Statistical analysis also showed significant differences between NIDCM and HCM groups for all approaches except midventricular SAX and midventricular-basal septal measurements (Table 3).

There was no statistically significant difference between SAX and septal measurements for 3 slice levels for each study group ($P > .05$). The mean T1 values compared between SAX and septal measurements in 3 slices showed a statistically significant correlation ($r = 0.921$, $P < .001$, $r = 0.948$, $P < .001$, and $r = 0.921$, $P < .001$, respectively) (Figure 4).

Coefficient of variation values, the heterogeneity of native T1 measures, were significantly higher for SAX measurements (basal: 0.060 ± 0.015, midventricular: 0.057 ± 0.016, apical: 0.056 ± 0.017) than septal ROIs (basal: 0.048 ± 0.013, midventricular: 0.048 ± 0.089, apical: 0.039 ± 0.012) ($P < .001$). Also, CoV values were significantly higher in NIDCM group than control group for all measures. The spread of differences was higher for the NIDCM group than the HCM

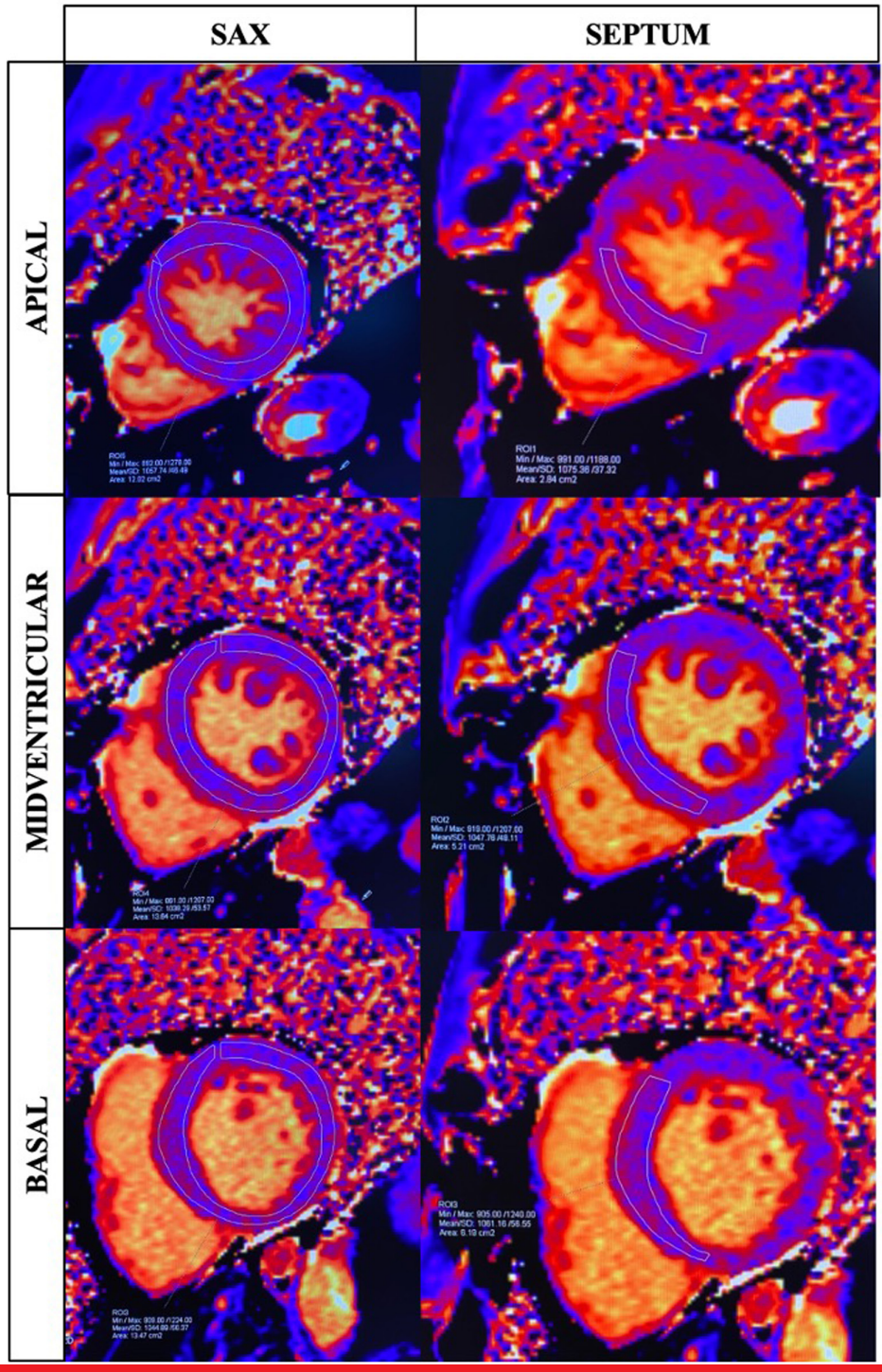

Figure 3. Native T1 mapping measurement techniques. ROIs were drawn manually within the whole LV myocardium (SAX) and interventricular septum in 3 different slices for the calculation of the mean myocardial T1 value. LV, left ventricle; ROI, region of interest; SAX, short-axis.

group, and also for the control group than the HCM group (Table 4).

Receiver operating characteristic curve analysis with corresponding cut-off values between study groups for each native T1 measurement approach is shown in Table 5. Figure 5 illustrates ROC curves of native T1 values for the differentiation of cardiomyopathies compared to controls and between cardiomyopathies. The NIDCM group had higher diagnostic accuracy compared to the HCM group [(75.9%-86%) vs. (66.7%-73.45%), respectively]. Basal SAX and basal septal measurements provided the highest diagnostic accuracy values and AUC for both cardiomyopathy groups; however, none of these differences were

Table 1. Demographic Characteristics of Study Groups

	Control (n = 22)	NIDCM (n = 61)	HCM (n = 60)
Age (Years)	38.3 ± 13.3	43 ± 14.7	48.2 ± 14.1*
Male	13 (65 %)	38 (62.3 %)	43 (70.5 %)
Weight (kg)	81 ± 11.7	79.6 ± 16.2	81.6 ± 14.9
Height (m)	1.73 ± 0.1	1.71 ± 0.2	1.69 ± 0.1
BMI (kg/m^2)	27.2 ± 3.8	26.5 ± 6.2	28.4 ± 4.3
BSA (m^2)	1.94 ± 0.2	1.87 ± 0.2	1.92 ± 0.2

Values are presented as mean ± SD and/or n (%). Continuous variables were compared across the 3 groups using one-way ANOVA or the Kruskal–Wallis test, as appropriate. p-values for pairwise comparisons were derived from Tukey's HSD test or the Bonferroni-corrected Dunn's test, depending on the normality of the data distribution.
*indicates statistical significance ($P < .05$) vs control.
BMI, body mass index; BSA, body surface area; HCM, hypertrophic cardiomyopathy; NIDCM, nonischemic dilated cardiomyopathy; SD, standard deviation.

significant. The details of diagnostic performance of native T1 mapping according to the cut-off values are presented in Table 6.

Analysis of Correlations

T1 values showed negative correlation with LV-EF and positive correlation with LV-EDVi and indexed LV mass. There was no statistically significant correlation between LVWTmax and T1 values for any of the measurement approaches, including all subjects. However, in HCM patients, there was a positive correlation between LVWTmax and T1 values (Table 7). Also in NIDCM patients, statistical analysis showed a weak negative correlation between LVWTmax and T1 values in apical SAX and septal measurements ($r = -0.252$, $P = .025$; $r = -0.273$, $P = .017$, respectively).

In 39 patients (60.9%) with NIDCM and 51 patients (79.6%) with HCM, visually detectable LGE was found in at least 1 segment. T1 values were significantly higher in cardiomyopathies with the LGE subgroup compared with controls. Statistical analysis showed no significant difference in T1 values between cardiomyopathies with and without LGE. T1

Table 2. Global Morphological and Functional Parameters of Study Groups

	Control (n = 22)	NIDCM (n = 61)	HCM (n = 60)
LV-EF (%)	59.8 ± 5.8	31.5 ± 10.1*	*63 ± 11.6*
LV-ESVi (mL/m^2)	28.9 ± 8	*88.8 ± 31.5**	*25.4 ± 12.2*
LV-EDVi (mL/m^2)	70.8 ± 12	*127.7 ± 29.4**	*67.2 ± 18.2*
LV-Mass index (g/m^2)	60.1 ± 10	*88.4 ± 20.5**	*96 ± 32.4**
LVWTmax (mm)	9.6 ± 1.9	*8.7 ± 2.2*	*22.3 ± 5.7**

Values are presented as mean ± SD. Due to the non-normal distribution of the data, global comparisons were performed using the Kruskal–Wallis test ($df = 2$), and adjusted p-values for pairwise comparisons were derived from the Bonferroni-adjusted Dunn's test.
*$P < .05$ indicates statistical significance vs control; italic values represent $P < .05$ indicates statistical significance between NIDCM and HCM.
EF, ejection fraction; EDV, end-diastolic volume; ESV, end-systolic volume; HR, heart rate; LV, left ventricle; LVWTmax, maximal wall thickness; SD, standard deviation.

Table 3. Native T1 Relaxation Times in Controls, NIDCM, and HCM Groups

	Control	NIDCM	Adj. *P*	Control	HCM	Adj. *P*	NIDCM	HCM	Adj. *P*
Native T1 relaxation times (ms)									
SAX									
Apical	996.1 ± 23.1	1053.3 ± 60.1	<.001*	996.1 ± 23.1	1025.4 ± 46.7	0.009*	1053.3 ± 60.1	1025.4 ± 46.7	.008*
Midventricular	996.8 ± 25.8	1046.7 ± 55.6	<.001*	996.8 ± 25.8	1026.9 ± 43.4	0.007*	1046.7 ± 55.6	1026.9 ± 43.4	.097
Basal	995.8 ± 20.8	1048.7 ± 53.3	<.001*	995.8 ± 20.8	1026.3 ± 41.1	0.003*	1048.7 ± 53.3	1026.3 ± 41.1	.008*
Septum									
Apical	999.9 ± 25.6	1062.1 ± 67.5	<.001*	999.9 ± 25.6	1034.2 ± 52.2	0.007*	1062.1 ± 67.5	1034.2 ± 52.2	.033*
Midventricular	1002.5 ± 26.6	1056.4 ± 55.7	<.001*	1002.5 ± 26.6	1036.6 ± 50.7	0.003*	1056.4 ± 55.7	1036.6 ± 50.7	.180
Basal	994.9 ± 22.9	1054 ± 60	<.001*	994.9 ± 22.9	1030.6 ± 44.3	0.003*	1054 ± 60	1030.6 ± 44.3	.610

Values are presented as mean ± SD. Due to the non-normal distribution of the data, global comparisons were performed using the Kruskal–Wallis test ($df = 2$), and adjusted p-values for pairwise comparisons were derived from the Bonferroni-adjusted Dunn's test.
*$P < .05$ indicates statistical significance.
Adj, adjusted; HCM, hypertrophic cardiomyopathy; NIDCM, nonischemic dilated cardiomyopathy; SD, standard deviation; SAX, short-axis.

values were significantly higher in cardiomyopathies without LGE subgroup compared to controls (Figure 6).

Assessment of Reproducibility and Agreement of Native T1 Mapping

In a subset of subjects (n = 31), excellent intraobserver was demonstrated (SAX: apical = 0.980, midventricular = 0.992, basal = 0.985; Septal: apical = 0.989, midventricular = 0.991, basal = 0.963; $P < .001$ for all) and interobserver (SAX: apical = 0.979, midventricular = 0.986, basal = 0.984; Septal: apical = 0.981, midventricular = 0.990, basal = 0.991; $P < .001$ for all) agreement in T1 values for each measurement approach.

DISCUSSION

In this retrospective case-control study, native T1 mapping demonstrated excellent diagnostic performance in differentiating healthy myocardium from diffuse disease in both NIDCM and HCM cohorts, yielding consistently high

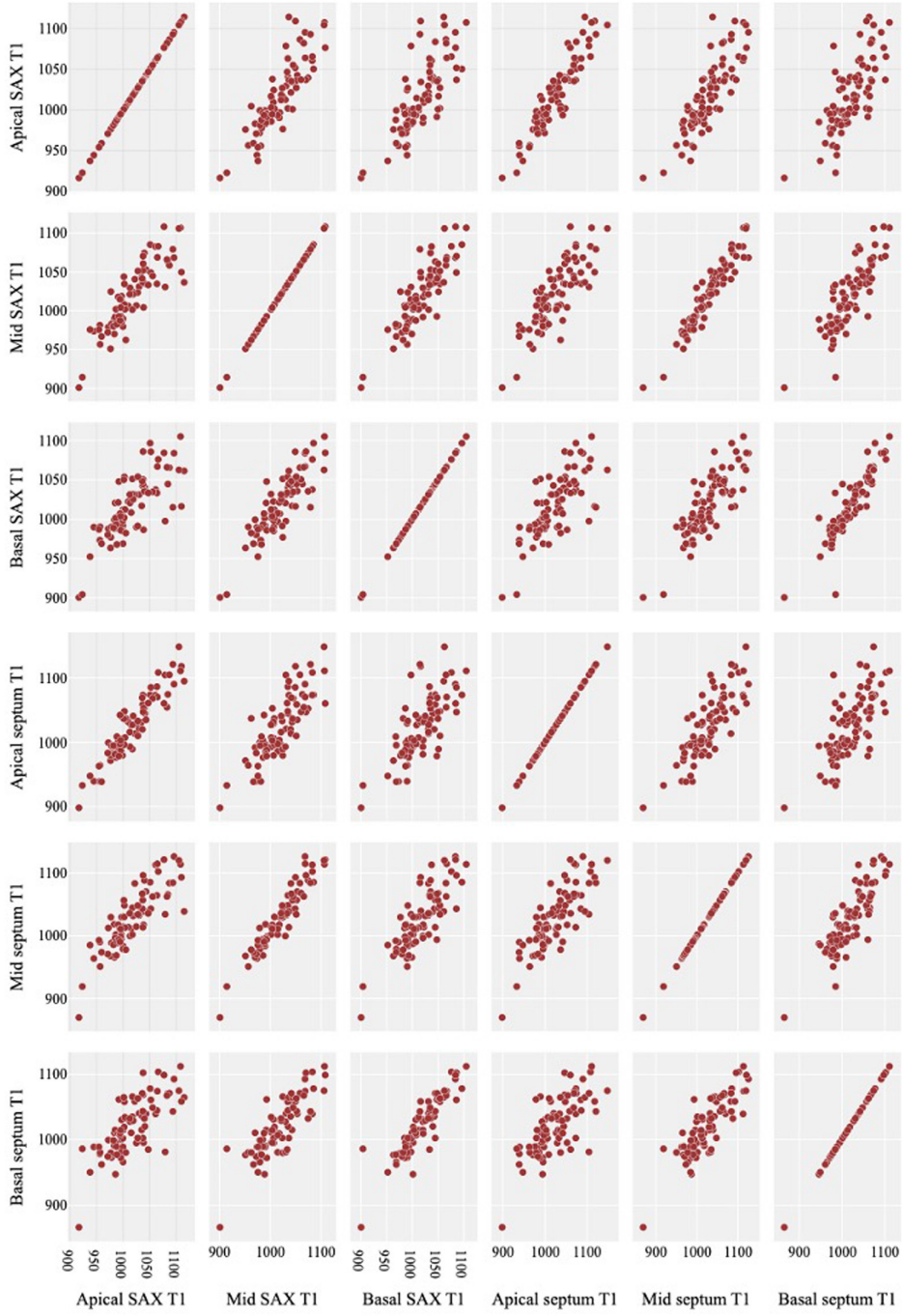

Figure 4. Correlation between different measurement techniques. Scatter plot diagrams, comparing the native T1 values between different measurement techniques for all subjects. Values are presented as mean (ms). ms, millisecond; SAX, short-axis.

Table 4. Comparison of Heterogeneity of Native T1 Values (CoV) Between Study Groups for Each Measurement Technique

	Control (n = 22)	NIDCM (n = 61)	Adj. *P*	Control (n = 22)	HCM (n = 60)	Adj. *P*	NIDCM (n = 61)	HCM (n = 60)	Adj. *P*
CoV									
SAX									
Apical	0.042 ± 0.014	0.064 ± 0.018	<.001*	0.042 ± 0.014	0.053 ± 0.012	.001*	0.064 ± 0.018	0.053 ± 0.012	.001*
Midventricular	0.044 ± 0.015	0.065 ± 0.015	<.001*	0.044 ± 0.015	0.054 ± 0.013	.005*	0.065 ± 0.015	0.054 ± 0.013	<.001*
Basal	0.049 ± 0.010	0.068 ± 0.014	<.001*	0.049 ± 0.010	0.057 ± 0.016	.014*	0.068 ± 0.014	0.057 ± 0.016	<.001*
Septum									
Apical	0.032 ± 0.010	0.041 ± 0.012	<.001*	0.032 ± 0.010	0.039 ± 0.012	.002*	0.041 ± 0.012	0.039 ± 0.012	.558
Midventricular	0.035 ± 0.009	0.045 ± 0.014	<.001*	0.035 ± 0.009	0.039 ± 0.009	.018*	0.045 ± 0.014	0.039 ± 0.009	.093
Basal	0.040 ± 0.011	0.051 ± 0.014	<.001*	0.040 ± 0.011	0.047 ± 0.012	.018*	0.051 ± 0.014	0.047 ± 0.012	.391

Values are presented as mean ± SD. Due to the non-normal distribution of the data, global comparisons were performed using the Kruskal–Wallis test ($df = 2$), and adjusted p-values for pairwise comparisons were derived from the Bonferroni-adjusted Dunn's test.
* $P < .05$ indicates statistical significance.
Adj, adjusted; CoV, coefficent of variation; HCM, hypertrophic cardiomyopathy; NIDCM, nonischemic dilated cardiomyopathy; SAX, short-axis.

AUC values without the need for contrast administration. A primary finding of the investigation is that a single-slice acquisition alone provides diagnostic accuracy comparable to multi-slice protocols. While the basal slice, both SAX and septum, demonstrated the numerically highest AUC values, no statistically significant difference was observed across the different ventricular levels. This lack of significant variance suggests that a standardized single-slice acquisition alone is sufficient for reliable diagnosis, effectively streamlining the imaging process and enhancing clinical workflow without compromising diagnostic performance.

While myocardial T1 measurement approaches vary significantly in literature, ranging from 16-segment models to whole-slice analysis, identifying a standardized and reproducible technique remains a cornerstone for clinical implementation. The interventricular septum is recommended for measurements due to its high prevalence of fibrosis, the lack of susceptibility artifacts from the lung, liver, and venous structures, and the reduced partial-volume effects.[7,10,27,28] Furthermore, the SCMR and the EACVI consensus statement currently recommend a single ROI in the mid-cavity septum.[10] The stability of septal-focused sampling is further corroborated by the ConSept study (1.5 T and 3 T MOLLI, 43 DCM, 25 LV hypertrophy, 38 controls), which directly compared septal versus whole SAX ROIs.[14] Their results indicated that septal ROIs showed lower intra-observer, inter-observer, and inter-study variability, while offering the greatest discrimination between healthy and diseased myocardium. Similarly, multicenter MOLLI trials have used standardized septal approaches to achieve excellent cross-center consistency despite significant regional variation in T1 values across different segments.[32]Consistent with these studies, the findings strongly support the septal approach and highlight its practical applications. Previous studies have also established that segmental measurement methods reveal significant variation in T1 values across the myocardium, with the greatest variability observed in the lateral segments and the least in the septal regions.[7,14,29-30] Similarly, the demonstrated T1 measurement heterogeneity, expressed as CoV, was significantly higher for SAX measurements compared to septal ROIs ($P < .001$). This finding is related to the fact that the SAX approach is a combination of all T1 values observed in the entire SAX slice and therefore includes T1 values of lateral segments, which show significantly higher variability than the septum. Lateral wall sampling has a high probability of including voxels outside the myocardium, or the partial volumes of interspersed voxels at the myocardium-blood or myocardium-lung interfaces, leading to mixed T1 signals.[14]

The results revealed basal SAX and basal septal measurements yielded the highest AUC values for both NIDCM and HCM cohorts. While this numerically superior performance at the basal level might be attributed to higher regional wall stress and early-stage remodeling frequently observed in these segments, it is important to note that these values were statistically comparable to the mid-ventricular level recommended by the SCMR/EACVI guidelines and previous studies. [10,31-34] This observation aligns with recent studies that include basal slices in comprehensive protocols. Specific

Table 5. Cut-Off Values from ROC Curve Analysis of Native T1 Relaxation Times for Each Measurement Technique Between Study Groups

	Cut-Off	AUC	*P*	95% CI
Cut-off values from ROC curve analysis of native T1 values in control group and NIDCM				
T1 SAX				
Apical	1016	0.864	<.001*	0.786-0.943
Midventricular	1019.42	0.831	<.001*	0.744-0.917
Basal	1013.41	0.885	<.001*	0.810-0.960
T1 SEPTUM				
Apical	1022.86	0.840	<.001*	0.756-0.923
Midventricular	1032.94	0.843	<.001*	0.761-0.924
Basal	1016.8	0.844	<.001*	0.761-0.928
Cut-off values from ROC curve analysis of native T1 values in control group and HCM				
T1 SAX				
Apical	1000.76	0.723	.002*	0.614-0.833
Midventricular	1020.28	0.720	.002*	0.612-0.829
Basal	1012.41	0.750	.001*	0.647-0.854
T1 SEPTUM				
Apical	1003.86	0.737	.001*	0.632-0.841
Midventricular	1013.1	0.729	.002*	0.622-0.836
Basal	1010.56	0.755	<.001*	0.653-0.856
Cut-off values from ROC curve analysis of native T1 values in NIDCM and HCM				
T1 SAX				
Apical	1040.9	0.661	.002*	0.564-0.759
Midventricular	1041.67	0.613	.032*	0.513-0.714
Basal	1038.13	0.662	.002*	0.565-0.759
T1 SEPTUM				
Apical	1048.87	0.640	.008*	0.541-0.738

Values are presented as mean ± SD. ROC curve analysis was only performed for parameters that demonstrated statistically significant differences between groups in the initial comparative analysis. Parameters with $P > .05$ were excluded from ROC analysis due to lack of diagnostic discriminatory power.
*$P < .05$ indicates statistical significance.
AUC, area under curve; HCM, hypertrophic cardiomyopathy; NIDCM, nonischemic dilated cardiomyopathy; ROC, receiver operating characteristic; SAX, short-axis.

studies focusing on Fabry-like and hypertrophic phenotypes have explicitly proposed the basal septum as a highly appropriate region for native T1 measurements, citing its lower SD and superior discriminative power in differentiating various hypertrophic phenotypes.[35,36] Additionally, some investigations focusing on Duchenne muscular dystrophy and hemodialysis cohorts have shown that basal T1 values exhibit high diagnostic performance and reproducibility, comparable to mid-level measurements.[37-38] However, despite these findings, current literature indicates that there is still a lack of standalone recommendations for using a single-slice basal approach as the primary diagnostic standard. Nevertheless, these values are usually used as supplementary data rather than as a standalone alternative.[10,34,39]

Critically, since no statistically significant difference in diagnostic accuracy was observed between the 3 ventricular levels, and septal measurements demonstrated significantly lower measurement heterogeneity than whole-slice SAX approaches, it is argued that a standardized, single-slice acquisition at 1 level, using a septal measurement method, is a robust and sufficient approach for reliable diagnosis. Transitioning toward a single-slice method could significantly enhance clinical workflow and reduce the cumulative breath-holding burden on patients without compromising the diagnostic performance of native T1 mapping. This practical optimization is essential for the further standardization and procedural efficiency of T1 mapping in routine clinical practice, where minimizing examination time and maximizing patient compliance are crucial. In addition to improving process efficiency, the adoption of a standardized single-slice approach is essential for minimizing both intra- and inter-observer variability. Performing all mapping measurements at a consistent anatomical level for each patient, such as the basal or mid-ventricular region, is crucial for ensuring longitudinal comparability. This standardization enables highly reproducible follow-up assessments across imaging sessions and among different readers, which is necessary for accurate monitoring of disease progression or therapeutic response in cardiomyopathies.

T1 values correlate with measures of global systolic function and LV remodeling. The findings agree with Puntmann et al[7] who conducted research (3 T MOLLI; 27 NIDCM, 25 HCM, 30

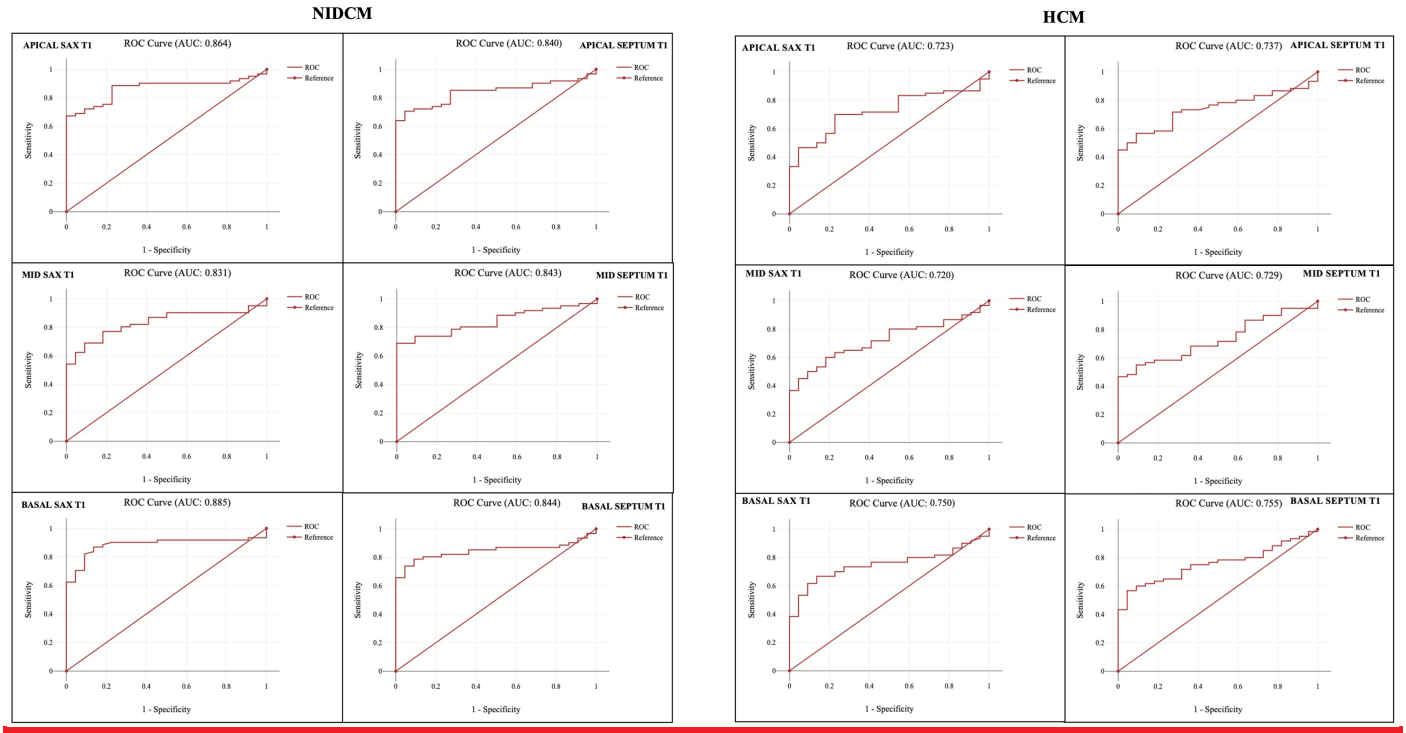

Figure 5. ROC curve of native T1 relaxation times for each measurement technique for the diagnosis of NIDCM and HCM. *$P < .05$ indicates statistical significance. AUC, area under curve; HCM, hypertrophic cardiomyopathy; NIDCM, nonischemic dilated cardiomyopathy; ROC, receiver operating characteristic; SAX, short-axis.

control subjects) and showed that T1 values have a negative correlation with LV-EF and a positive correlation with indexed LV-EDV.

In HCM patients, it was observed that T1 values have a positive correlation with LVWTmax for all measurement approaches. Similarly, Hinojar et al[40] [(3 T MOLLI ((3(3)3(3)5); 95 HCM and 32 controls] who reported a similar association between T1 and both indexed LV mass ($r = 0.47$, $P < .001$) and LVWTmax ($r = 0.44$, $P < .001$). In another study, Puntmann et al[7] (3 T MOLLI; 27 NIDCM, 25 HCM, 30 control subjects) found a positive association between T1 and indexed LV mass ($r = 0.51$, $P < .001$) in patients with HCM. Studies on HCM using segmental analysis of standard American Heart Association (AHA) segments have demonstrated that hypertrophied or LGE-positive segments exhibit higher native T1 values than non-hypertrophied or LGE-negative segments. These findings support the use of focal interrogation of diseased segments as a complementary approach to, rather than an alternative for, global assessment.[27,41] However, the current literature does not specify the requirement for subtype-specific measurement techniques for different HCM phenotypes.[42,43] The study did not perform a subgroup analysis based on specific HCM phenotypes and did not specifically target hypertrophied segments for ROI placement. The results indicate that even a simplified single-slice approach with whole-SAX or septal measurements effectively distinguishes pathological myocardium and reflects the degree of hypertrophy, consistent with previous studies.[7,40] These findings indicate that the streamlined method effectively captures the systemic myocardial involvement characteristic of HCM, although it may be less sensitive in detecting peak regional values in complex phenotypes compared to comprehensive segmental mapping.

In NIDCM patients, statistical analysis revealed a weak negative correlation between LVWTmax and T1 values only in apical SAX and septal measurements. It is assumed that this finding is mainly related to measurement errors due to the more difficult and artifact-prone apical measurements.

A total of 90 patients (39 NIDCM and 51 HCM) showed at least 1 segment of visually detectable LGE. Cardiomyopathies with LGE showed higher T1 values than the control group. However, T1 relaxation times were significantly longer even in cardiomyopathies without the LGE subgroup compared to controls. In the current study, there was no significant difference in T1 values between cardiomyopathies with and without LGE. This finding is in agreement with a study performed by Puntmann et al[7] (3 T MOLLI; 27 NIDCM, 25 HCM, 30 control subjects) that showed that there were no significant differences in mean T1 values between subjects with visually detectable LGE and those without it. Dass et al[27] (3 T ShMOLLI; 18 DCM, 28 HCM, 12 control subjects) demonstrated that in HCM and DCM patients T1 values were significantly higher in segments with LGE than in those without it, even in segments not demonstrating LGE T1 values were significantly higher than normal for each patient group. In another study, Elsafty et al[30] (1.5 T LL; 50 DCM, 12 HCM, 10 healthy volunteers) reported that including all patients, T1 values were significantly higher in segments with LGE than in those without it, even in segments not demonstrating LGE T1

Table 6. The Diagnostic Performance of Native T1 Mapping for Each Measurement Technique According to the Presented Cutt-Off Values

	TP	TN	FP	FN	Sensitivity			Specificity			Accuracy	PPV		NPV	
	(n)	(n)	(n)	(n)	(n)	%	95% CI	(n)	%	95% CI	%	%	95% CI	%	95% CI
Native T1 values for differentiating control group and NIDCM															
SAX															
Apical	47	19	5	15	47/62	75.8	63.8-84.8	19/24	79.2	59.5-90.8	76.7	90.4	81.6-95.4	55.9	44.8-66.4
Midventricular	49	23	5	14	49/63	77.8	66.1-86.3	23/28	82.1	64.4-92.1	79.1	90.7	82.4-95.5	62.2	51.3-71.9
Basal	55	25	5	8	55/63	87.3	76.9-93.4	25/30	83.3	64.4-92.7	86	91.7	83.6-96.1	75.8	65.6-83.8
Septum															
Apical	47	19	6	15	47/62	75.8	63.8-84.8	19/25	76	56.6-88.5	75.9	88.7	79.6-94.2	55.9	44.9-66.4
Midventricular	47	26	3	16	47/63	74.6	62.7-83.7	26/29	89.7	73.6-96.4	79.3	94	86.5-97.6	61.9	51.1-71.7
Basal	50	25	4	12	50/62	80.6	69.1-88.6	25/29	86.2	69.4-94.5	82.4	92.6	84.6-96.8	67.6	56.8-76.8
Native T1 values for differentiating control group and HCM															
SAX															
Apical	43	18	6	18	43/61	70.5	58.1-80.4	18/24	75	55.1-88	71.8	87.8	78.4-93.6	50	39-61
Midventricular	37	23	5	25	37/62	59.7	47.3-71	23/28	82.1	64.4-92.1	66.7	88.1	79.1-93.7	47.9	37.4-58.6
Basal	44	25	5	20	44/64	68.8	56.6-78.8	25/30	83.3	64.4-92.7	73.4	89.8	81.4-94.8	55.6	45-65.7
Septum															
Apical	44	18	7	17	44/61	72.1	59.8-81.8	18/25	72	52.4-85.7	72.1	86.3	76.8-92.4	51.4	40.5-62.3
Midventricular	43	18	11	19	43/62	69.4	57-79.4	18/29	62.1	44-77.3	67	79.6	69.6-87.1	48.6	38.1-59.3
Basal	42	21	8	21	42/63	66.7	54.4-77.1	21/29	72.4	54.3-85.3	68.5	84	74.6-90.5	50	39.5-60.5
Native T1 values for differentiating NIDCM and HCM															
SAX															
Apical	41	41	20	21	41/62	66.1	53.7-76.7	41/61	67.2	54.7-77.7	66.7	67.2	58.1-75.2	66.1	57-74.3
Midventricular	38	39	23	25	38/63	60.3	48-71.5	39/62	62.9	50.5-73.8	61.6	62.3	53.1-70.7	60.9	51.8-69.4
Basal	42	40	24	21	42/63	66.7	54.4-77.1	40/64	62.5	50.3-73.3	64.6	63.6	54.6-71.9	65.6	56.6-73.6
Septum															
Apical	38	37	24	24	38/62	61.3	48.8-72.4	37/61	60.7	48.1-71.9	61	61.3	52.1-69.8	60.7	51.4-69.2
Basal	40	39	24	22	40/62	64.5	52.1-75.3	39/63	61.9	49.6-72.9	63.2	62.5	53.4-70.9	63.9	54.8-72.2

*$P < .05$ indicates statistical significance.

FN, false negative; FP, false positive; HCM, hypertrophic cardiomyopathy; NIDCM, nonischemic dilated cardiomyopathy; NPV, negative predictive value; PPV, positive predictive value; SAX, short-axis; TN, true negative; TP, true positive.

Table 7. Spearman Correlation Between Native T1 Relaxation Times and LV-EF. LV-EDVi and LV-Mass Index Including All Subjects and Spearman Correlation Between Native T1 Relaxation Times and LVWTmax and LV-Mass Index for HCM Patients

LV-EF All Subjects		
	r	***P***
T1 SAX		
Apical	−0.284	<.001*
Midventricular	−0.226	.005*
Basal	−0.291	<.001*
T1 SEPTUM		
Apical	−0.273	.001*
Midventricular	−0.198	.014*
Basal	−0.229	.004*
LV-EDVi All Subjects		
	r	*P*
T1 SAX		
Apical	0.367	<.001*
Midventricular	0.308	<.001*
Basal	0.350	<.001*
T1 SEPTUM		
Apical	0.348	<.001*
Midventricular	0.288	<.001*
Basal	0.308	<.001*
LV-Mass Index All Subjects		
	r	*P*
T1 SAX		
Apical	0.141	.095*
Midventricular	0.285	<.001*
Basal	0.286	<.001*
T1 SEPTUM		
Apical	0.192	.021*
Midventricular	0.286	<.001*
Basal	0.274	.001*

HCM GROUP	LVWTmax		LV Mass Index	
	r	*P*	*r*	*P*
T1 SAX				
Apical	0.349	.003*	0.041	.381
Midventricular	0.398	.001*	0.224	.047*
Basal	0.409	.001*	0.173	.099
T1 SEPTUM				
Apical	0.374	.002*	0.005	.516
Midventricular	0.372	.002*	0.139	.151
Basal	0.400	.001*	0.131	.166

*$P < .05$ indicates statistical significance.
EF, ejection fractio; EDVi, end-diastolic volume index; LV, left ventricle; LVWTmax, maximal left ventricular wall thickness; SAX, short-axis.

values were significantly higher than normal. It appears that the explanation for this difference between the mentioned studies and this study is the segmental measurement technique. Dass et al[27] and Elsafty et al[30] performed segmental measurements of T1 values and compared T1 values with the effect of the presence of segmental LGE. However, the effect of LGE presence was investigated at any segment on overall myocardial T1 values.

T1 mapping was found to be a powerful method for differentiating between NIDCM and controls with high sensitivity, specificity, diagnostic accuracy, and positive predictive value (PPV), but not for negative predictive value (NPV). For differentiating HCM from controls, the mean T1 was found to have relatively good sensitivity, specificity, accuracy, and PPV compared to the NIDCM group, but it also has limited NPV. Thongsongsang et al[44] (3 T 5(3)3 MOLLI; 157 DCM, 112 HCM, 595 controls) reported a significant difference in the mean T1 values of midventricular SAX and septum compared to the control group with DCM and HCM patients. Their study's AUC results are similar to the study. The number of patients and the variety in field strength they used could explain the difference in specificity and NPV of T1 values. This study observed a lower sensitivity, specificity, and AUC than Puntmann et al.[7] Rogers et al[14] reported that T1 values showed significant differences between controls and LV hypertrophy and DCM groups for both septal and SAX measurement techniques, with greater differences observed at 3 T compared to 1.5 T field strength. Therefore, it is believed that this difference may be explained by the different imaging platforms that Puntmann et al[7] used.

The possible reason for higher T1 values and AUC results in NIDCM patients compared to HCM in the study as well as in the previously cited studies could be related to the thin-walled myocardium in NIDCM cases, which is subject to a potential measurement error related to partial volume effect.[29,45] The study further showed that CoV values were significantly higher in NIDCM group than control group for all measures. While increased wall thickness obviously improves ROI placement within the myocardium, the potential for measurement error in the thinned, dilated myocardium is significantly higher. The spread of differences was also higher for the control group than the HCM group. The recorded regional differences are unlikely to represent a real difference in tissue composition. Instead, the reported differences are thought to be caused by some other factors, such as magnetic susceptibility artifacts and measurement errors related to wall thickness.

Goebel et al[28] (1.5 T 5(3)3 MOLLI; 17 DCM, 12 HCM, 54 healthy hearts) reported a significant difference in mean T1 values between healthy heart subjects with DCM and HCM patients. The AUC for the DCM group was 0.814 ($P < .001$), and the AUC for the HCM group was 0.688 ($P = .067$). Badr et al[46] (1.5 T MOLLI; 30 DCM, 15 healthy participants) recorded an AUC value of 0.919 for differentiating between myocardial fibrosis in the DCM group and normal myocardium in healthy controls. Both of the mentioned studies performed T1 mapping on a 1.5 T MRI system with MOLLI sequence, and their results are similar to the AUC results of the study.

Regarding the reliability of T1 values, Puntmann et al[7] and Badr et al[46] found excellent inter-observer agreement for T1 estimation with ICC of 0.98 and 0.928, respectively, which

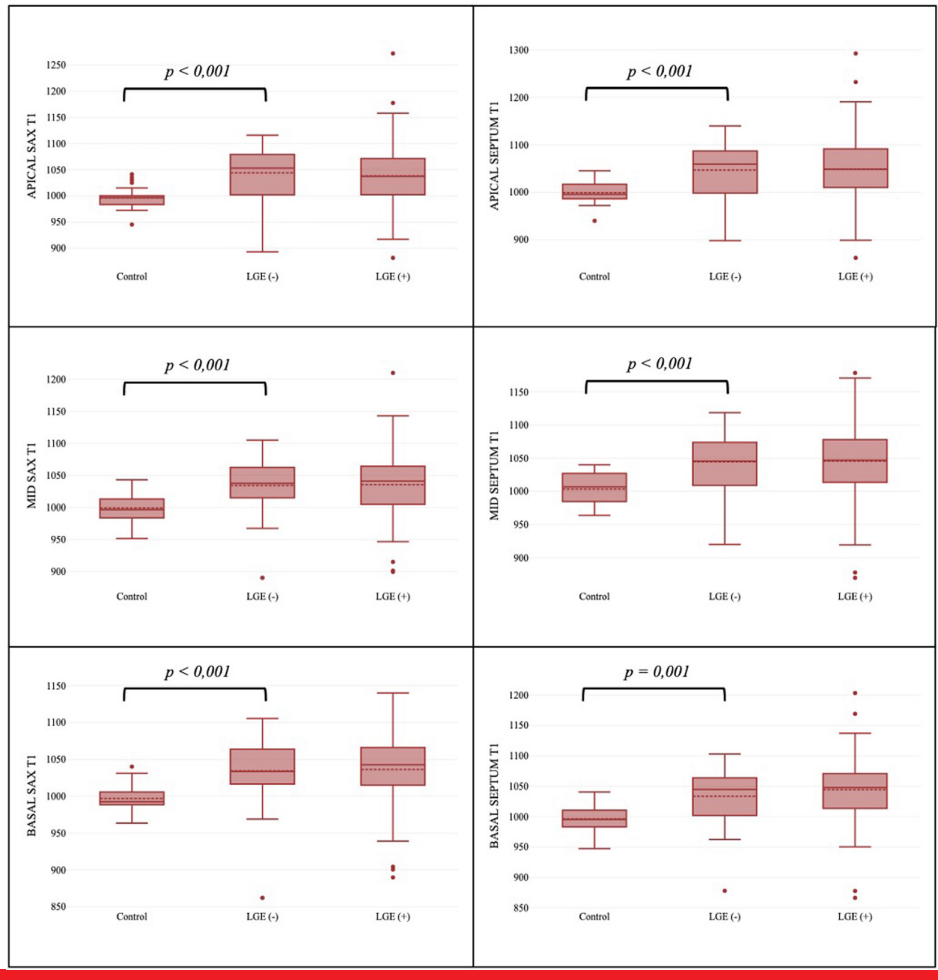

Figure 6. Comparison of native T1 relaxation times between the control group and cardiomyopathies with and without LGE subgroups. *$P < .05$ indicates statistical significance. LGE, late gadolinium enhancement; SAX, short-axis.

are consistent with the study (minimum 0.979 and maximum 0.986 for SAX measurements; minimum 0.981 and maximum 0.991 for septal measurements). As a result, the T1 mapping technique is considered to be a reproducible imaging method, regardless of the measurement technique.

Limitations of the Study

This study has some notable limitations. First, it was conducted with a relatively small sample size at a single center. Second, the prolonged acquisition time, its heart-rate dependence, and motion artifacts can all lead to errors in the pixel-based estimation of T1 values.[47] By using the MOLLI 5(3)3 sequence and also motion and heart-rate correction algorithms, it is believed that most of these effects have been minimized.[48] Third, the study was conducted over a 7-year period, which could introduce variability resulting from minor scanner software updates.This potential source of variability was addressed by maintaining consistent imaging parameters and employing a concurrent internal control group that was temporally matched to the patient cohorts. This approach ensured longitudinal stability. Fourth, clinical practicality was prioritized by utilizing whole-myocardial and septal ROI approaches instead of a segmental method. Consequently, the cohort was not stratified by specific HCM phenotypes and did not specifically target hypertrophied segments for ROI placement, which may limit the detection of peak regional T1 heterogeneity in patients with highly localized hypertrophy. However, the objective was to establish a more efficient workflow for routine clinical practice. Finally, because native T1 values are vendor-specific, the thresholds reported in this study may not be directly applicable to other platforms or sequences.

CONCLUSION

In conclusion, consistent with the existing literature, native T1 mapping provides high diagnostic accuracy and excellent reproducibility for assessing myocardial fibrosis in NIDCM and HCM patients. The findings confirm that native T1 values can detect myocardial involvement at an early stage, even before fibrosis is visible on LGE imaging, making it a valuable contrast-free technique, particularly for patients with contraindications to gadolinium-based contrast agents. Beyond these established clinical benefits, the primary contribution of the study is the demonstration that a streamlined, single-slice acquisition, combined with the septal measurement technique, offers diagnostic performance comparable to multi-slice protocols while providing lower measurement

heterogeneity. This optimization enables a more time-efficient diagnostic process without compromising clinical confidence.

Ethics Committee Approval: We declare that this retrospective study has been approved by the Institutional Human Research Ethics Committee of Ankara University (Approval No: I01-65-24, dated February 6, 2024), and has therefore been performed in accordance with the ethical standards laid down in the 1964 Declaration of Helsinki and its later amendments.

Informed Consent: Written consent was obtained from the patients that their images could be used in scientific studies without sharing personal data or information that would reveal their identities.

Peer-Review: Externally peer-reviewed.

Declarations on AI Use: The authors declare that no artificial intelligence (AI)-assisted technologies (such as Large Language Models, chatbots, or image creators) were used in the preparation of this manuscript or the production of its content.

Author Contributions: Concept – S.B.U., E.P.; Design – S.B.U., S.U., E.P.; Supervision – E.P., C.U.; Resource – S.U., E.P., C.U.; Materials – S.B.U., E.P.; Data Collection and/or Processing – S.B.U., E.P.; Analysis and/or Interpretation – S.U., E.P.; Literature Search – S.B.U., S.U.; Writing – S.B.U., S.U.; Critical Reviews – E.P., C.U.

Declaration of Interests: The authors have no conflicts of interest to declare.

Funding: The authors declare that this study received no financial support.

REFERENCES

1. Gordon B, González-Fernández V, Dos-Subirà L. Myocardial fibrosis in congenital heart disease. *Front Pediatr*. 2022;10:965204. [CrossRef]
2. Gyöngyösi M, Winkler J, Ramos I, et al. Myocardial fibrosis: biomedical research from bench to bedside. *Eur J Heart Fail*. 2017;19(2):177-191. [CrossRef]
3. Mewton N, Liu CY, Croisille P, Bluemke D, Lima JA. Assessment of myocardial fibrosis with cardiovascular magnetic resonance. *J Am Coll Cardiol*. 2011;57(8):891-903. [CrossRef]
4. Jellis CL, Kwon DH. Myocardial T1 mapping: modalities and clinical applications. *Cardiovasc Diagn Ther*. 2014;4(2):126-137. [CrossRef]
5. Hwang SH, Choi BW. Advanced cardiac MR imaging for myocardial characterization and quantification: T1 mapping. *Korean Circ J*. 2013;43(1):1-6. [CrossRef]
6. Germain P, El Ghannudi S, Jeung MY, et al. Native T1 mapping of the heart - a pictorial review. *Clin Med Insights Cardiol*. 2014;8(suppl 4):1-11. [CrossRef]
7. Puntmann VO, Voigt T, Chen Z, et al. Native T1 mapping in differentiation of normal myocardium from diffuse disease in hypertrophic and dilated cardiomyopathy. *JACC Cardiovasc Imaging*. 2013;6(4):475-484. [CrossRef]
8. Rehwald WG, Fieno DS, Chen EL, Kim RJ, Judd RM. Myocardial magnetic resonance imaging contrast agent concentrations after reversible and irreversible ischemic injury. *Circulation*. 2002;105(2):224-229. [CrossRef]
9. Kim RJ, Wu E, Rafael A, et al. The use of contrast-enhanced magnetic resonance imaging to identify reversible myocardial dysfunction. *N Engl J Med*. 2000;343(20):1445-1453. [CrossRef]
10. Messroghli DR, Moon JC, Ferreira VM, et al. Clinical recommendations for cardiovascular magnetic resonance mapping of T1, T2, T2* and extracellular volume: a consensus statement by the Society for Cardiovascular Magnetic Resonance (SCMR) endorsed by the European Association for Cardiovascular Imaging (EACVI). *J Cardiovasc Magn Reson*. 2017;19(1):75. [CrossRef]
11. Puntmann VO, Peker E, Chandrashekhar Y, Nagel E. T1 mapping in characterizing myocardial disease: A comprehensive review. *Circ Res*. 2016;119(2):277-299. [CrossRef]
12. Iles L, Pfluger H, Phrommintikul A, et al. Evaluation of diffuse myocardial fibrosis in heart failure with cardiac magnetic resonance contrast-enhanced T1 mapping. *J Am Coll Cardiol*. 2008;52(19):1574-1580. [CrossRef]
13. Garg P, Saunders LC, Swift AJ, Wild JM, Plein S. Role of cardiac T1 mapping and extracellular volume in the assessment of myocardial infarction. *Anatol J Cardiol*. 2018;19(6):404-411. [CrossRef]
14. Rogers T, Dabir D, Mahmoud I, et al. Standardization of T1 measurements with MOLLI in differentiation between health and disease--the ConSept study. *J Cardiovasc Magn Reson*. 2013;15(1):78. [CrossRef]
15. Arbelo E, Protonotarios A, Gimeno JR, et al. 2023 ESC Guidelines for the management of cardiomyopathies. *Eur Heart J*. 2023;44(37):3503-3626. [CrossRef]
16. Elliott P, Andersson B, Arbustini E, et al. Classification of the cardiomyopathies: a position statement from the European Society of Cardiology Working Group on Myocardial and Pericardial Diseases. *Eur Heart J*. 2008;29(2):270-276. [CrossRef]
17. Maceira AM, Prasad SK, Khan M, Pennell DJ. Normalized left ventricular systolic and diastolic function by steady state free precession cardiovascular magnetic resonance. *J Cardiovasc Magn Reson*. 2006;8(3):417-426. [CrossRef]
18. Hänselmann A, Veltmann C, Bauersachs J, Berliner D. Dilatative Kardiomyopathien und non-compaction-Kardiomyopathie. *Herz*. 2020;45(3):212-220. [CrossRef]
19. Ommen SR, Mital S, Burke MA, et al. 2020 AHA/ACC guideline for the diagnosis and treatment of patients with hypertrophic cardiomyopathy: a report of the American College of Cardiology/American Heart Association joint committee on clinical practice guidelines. *J Am Coll Cardiol*. 2020;76(25):e159-e240. [CrossRef]
20. Zeng JT, Zhang YA, Ma TY, et al. Twin phenomena of hypertrophic cardiomyopathy: A reported case series. *Anatol J Cardiol*. 2024;28(11):513-522. [CrossRef]
21. International T1 mapping multicentre consortium. International T1 multicentre outcome CMR study. https://www.cardiac-imaging.org/t1-outcome-study.html
22. Puntmann VO, Carr-White G, Jabbour A, et al. T1-mapping and outcome in nonischemic cardiomyopathy: all-cause mortality and heart failure. *JACC Cardiovasc Imaging*. 2016;9(1):40-50. [CrossRef]
23. Puntmann VO. Why CMR webinar: introduction into scanning and planning for CMR. *YouTube* [website]. www.youtube.com/watch?v=54s1BkjDKJw. Accessed July 15, 2019
24. Tseng WYI, Su MYM, Tseng YHE. Introduction to cardiovascular magnetic resonance: technical principles and clinical applications. *Acta Cardiol Sin*. 2016;32(2):129-144. [CrossRef]
25. Schildt JV, Loimaala AJ, Hippeläinen ET, Ahonen AA. Heterogeneity of myocardial 2-[18F]fluoro-2-deoxy-D-glucose uptake is a typical feature in cardiac sarcoidosis: a study of 231 patients. *Eur Heart J Cardiovasc Imaging*. 2018;19(3):293-298. [CrossRef]
26. Tahara N, Tahara A, Nitta Y, et al. Heterogeneous myocardial FDG uptake and the disease activity in cardiac sarcoidosis. *JACC Cardiovasc Imaging*. 2010;3(12):1219-1228. [CrossRef]

27. Dass S, Suttie JJ, Piechnik SK, et al. Myocardial tissue characterization using magnetic resonance noncontrast t1 mapping in hypertrophic and dilated cardiomyopathy. *Circ Cardiovasc Imaging*. 2012;5(6):726-733. [CrossRef]
28. Goebel J, Seifert I, Nensa F, et al. Can native T1 mapping differentiate between healthy and diffuse diseased myocardium in clinical routine cardiac MR imaging? *PLoS One*. 2016;11(5):e0155591. [CrossRef]
29. Piechnik SK, Ferreira VM, Dall'Armellina E, et al. Shortened Modified Look-Locker Inversion recovery (ShMOLLI) for clinical myocardial T1-mapping at 1.5 and 3 T within a 9 heartbeat breathhold. *J Cardiovasc Magn Reson*. 2010;12(1):69. [CrossRef]
30. Elsafty HG, El Shafey M, El Arabawy R, Mahrous MR, Dawoud TM. Could native T1 mapping replace late gadolinium enhancement in the assessment of myocardial fibrosis in patients with cardiomyopathy? *Egypt J Radiol Nucl Med*. 2021;52(1). [CrossRef]
31. Liu JM, Liu A, Leal J, et al. Measurement of myocardial native T1 in cardiovascular diseases and norm in 1291 subjects. *J Cardiovasc Magn Reson*. 2017;19(1):74. [CrossRef].
32. Dabir D, Child N, Kalra A, et al. Reference values for healthy human myocardium using a T1 mapping methodology: results from the International T1 Multicenter cardiovascular magnetic resonance study. *J Cardiovasc Magn Reson*. 2014;16(1):69. [CrossRef]
33. Haaf P, Garg P, Messroghli DR, Broadbent DA, Greenwood JP, Plein S. Cardiac T1 Mapping and Extracellular Volume (ECV) in clinical practice: a comprehensive review. *J Cardiovasc Magn Reson*. 2016;18(1):89. [CrossRef]
34. Radenkovic D, Weingärtner S, Ricketts L, Moon JC, Captur G. T1 mapping in cardiac MRI. *Heart Fail Rev*. 2017;22(4):415-430. [CrossRef]
35. Deborde E, Dubourg B, Bejar S, et al. Differentiation between Fabry disease and hypertrophic cardiomyopathy with cardiac T1 mapping. *Diagn Interv Imaging*. 2020;101(2):59-67. [CrossRef]
36. Sado DM, White SK, Piechnik SK, et al. Identification and assessment of Anderson-Fabry disease by cardiovascular magnetic resonance noncontrast myocardial T1 mapping. *Circ Cardiovasc Imaging*. 2013;6(3):392-398. [CrossRef]
37. Xu K, Xu HY, Xu R, et al. Global, segmental and layer specific analysis of myocardial involvement in Duchenne muscular dystrophy by cardiovascular magnetic resonance native T1 mapping. *J Cardiovasc Magn Reson*. 2021;23(1):110. [CrossRef]
38. Graham-Brown MP, Rutherford E, Levelt E, et al. Native T1 mapping: inter-study, inter-observer and inter-center reproducibility in hemodialysis patients. *J Cardiovasc Magn Reson*. 2017;19(1):21. [CrossRef]
39. Aherne E, Chow K, Carr J. Cardiac T1 mapping: techniques and applications. *J Magn Reson Imaging*. 2020;51(5):1336-1356. [CrossRef]
40. Hinojar R, Varma N, Child N, et al. T1 mapping in discrimination of hypertrophic phenotypes: hypertensive heart disease and hypertrophic cardiomyopathy: findings from the international T1 multicenter cardiovascular magnetic resonance study. *Circ Cardiovasc Imaging*. 2015;8(12):e003285. [CrossRef]
41. Wu CW, Wu R, Shi RY, et al. Histogram analysis of native T1 mapping and its relationship to left ventricular late gadolinium enhancement, hypertrophy, and segmental myocardial mechanics in patients with hypertrophic cardiomyopathy. *J Magn Reson Imaging*. 2019;49(3):668-677. [CrossRef]
42. Xu J, Zhuang B, Sirajuddin A, et al. MRI T1 mapping in hypertrophic cardiomyopathy: evaluation in patients without late gadolinium enhancement and hemodynamic obstruction. *Radiology*. 2020;294(2):275-286. [CrossRef]
43. Neisius U, El-Rewaidy H, Nakamori S, Rodriguez J, Manning WJ, Nezafat R. Radiomic analysis of myocardial native T1 imaging discriminates between hypertensive heart disease and hypertrophic cardiomyopathy. *JACC Cardiovasc Imaging*. 2019;12(10):1946-1954. [CrossRef]
44. Thongsongsang R, Songsangjinda T, Tanapibunpon P, Krittayaphong R. Native T1 mapping and extracellular volume fraction for differentiation of myocardial diseases from normal CMR controls in routine clinical practice. *BMC Cardiovasc Disord*. 2021;21(1):270. [CrossRef]
45. Reiter U, Reiter C, Kräuter C, Fuchsjäger M, Reiter G. Cardiac magnetic resonance T1 mapping. Part 2: Diagnostic potential and applications. *Eur J Radiol*. 2018;109:235-247. [CrossRef]
46. Badr SE, Gouhar GK, Zidan EH, et al. Can native T1 mapping sequence be used as a non-invasive alternative imaging tool to LGE sequence for evaluating DCM patients? *Egypt J Radiol Nucl Med*. 2024;55(1):8. [CrossRef]
47. Rogers T, Dabir D, Voigt T, Schaeffter T, Nagel E, Puntmann VO. Standardization of myocardial T1 time measurements in clinical setting using MOLLI, shMOLLI and LL at 1.5T and 3T - the CONSEPT study. *J Cardiovasc Magn Reson*. 2013;15(suppl 1):18. [CrossRef]
48. Diao KY, Yang ZG, Xu HY, et al. Histologic validation of myocardial fibrosis measured by T1 mapping: a systematic review and meta-analysis. *J Cardiovasc Magn Reson*. 2016;18(1):92. [CrossRef]